

LASER INTERFEROMETER GRAVITATIONAL WAVE OBSERVATORY  
- LIGO -  
CALIFORNIA INSTITUTE OF TECHNOLOGY  
MASSACHUSETTS INSTITUTE OF TECHNOLOGY

<b>Document Type</b> <b>LIGO-T970196-00 - E</b> Nov. 1997
<b>Physics of End-to-End model</b>
Biplab Bhawal, Matt Evans, Edward Maros, Malik Rahman and Hiro Yamamoto

*Distribution of this draft:*

xyz

This is an internal working note  
of the LIGO Project..

**California Institute of Technology**  
**LIGO Project - MS 51-33**  
**Pasadena CA 91125**  
Phone (626) 395-2129  
Fax (626) 304-9834  
E-mail: info@ligo.caltech.edu

**Massachusetts Institute of Technology**  
**LIGO Project - MS 20B-145**  
**Cambridge, MA 01239**  
Phone (617) 253-4824  
Fax (617) 253-7014  
E-mail: info@ligo.mit.edu

WWW: <http://www.ligo.caltech.edu/>

LIGO DRAFT



The field, in a particular polarization, is represented by a base of the mode representation and a mode amplitude vector, which is a vector of amplitudes for each eigen state:

$$E(x, y, z, t) = \exp(i\omega_0 t) \cdot \sum_{\sigma} \sum_{n, m=0}^{\text{max\_mn\_order}} E_{\sigma}^{mn}(z, t) \cdot U_{mn}(x, y, z) \quad (1)$$

$$E_{\sigma}^{mn}(z, t) = \exp(i\Omega_{\sigma} t - i(k_0 + k_{\sigma})z) \cdot \tilde{E}_{\sigma}^{mn}(t) \quad (2)$$

$$U_{mn}(x, y, z) = u_m(x, z) \cdot u_n(y, z) \quad (3)$$

$$u_m(x, z) = \sqrt{\frac{\sqrt{(2/\pi)}}{2^m m! W_x(z_x)}} H_m\left(\frac{\sqrt{2}x}{W_x(z_x)}\right) \exp\left(-x^2 \left(\frac{1}{W_x(z_x)^2} + \frac{ik}{2R(z_x)}\right) + i\left(m + \frac{1}{2}\right)\eta_{00}(z_x)\right) \quad (4)$$

An equation similar to Eq.(5) [i.e., replace m with n and x with y] describes  $u_n(y, z)$ . In these expressions, the index  $\sigma$  runs for all sidebands and a carrier. As is shown below, each field component of a field carries its own frequency, and there is no restriction among them. Strictly speaking, the wave number  $k = 2\pi/\lambda$  is calculated as  $k_0 + k_{\sigma}$ , where  $k_0$  is a reference wave number which is very close to or identical to that of the carrier, or  $k_{\sigma}/k_0 \sim \lambda_{CR}/\lambda_{SB} \sim 10^{-7}$ . The angular velocity and wave numbers are related as  $k_0 = \omega_0/c$ , and  $k_{\sigma} = \Omega_{\sigma}/c$ . In the simulation program,  $\tilde{E}_{\sigma}^{mn}(t)$  is kept as subfield components, and the phase change  $P_{\sigma}^{mn}(z)$  is calculated by the propagator.

So, the field in a particular polarization is represented by a set of  $U_{mn}$  and weights of each mode. The base of the Gaussian beam in E2E is thus represented by four quantities: Waist-sizes for the X- and Y- components of the beam,  $W_{x0}$ ,  $W_{y0}$  and distances of the waist positions,  $z_x$  and  $z_y$ . Note that these quantities for two transverse directions, X and Y, can change or evolve in an independent way. Table 1 describes some of the physical quantities for the light beam. The expressions of the quantities for X- and Y- components are of the same form and can be differentiated by adding subscript x or y to each of these quantities.

### 3.2. Change of Basis

When the base (represented by  $W_{x0}$ ,  $W_{y0}$ ,  $z_x$  and  $z_y$ ) is changed,  $U_{mn}$ 's change. When a field representation changes from one set of waist size and waist position to another set, it is called "the base of the field is changed". A field at a given location will carry the information of the representation base using the waist size and the distance to the waist position. The field going away from the waist position (diverging beam) will have positive distance, while that coming to the waist (converging beam) will have negative distance, just as is illustrated in Figure 1 [To keep the labels

**Table 1:**

<i>name</i>	<i>expression</i>	<i>size for LIGO</i>
mode-dependent Guoy phase shift	$\eta(z) = \tan^{-1}\left(\frac{z}{z_0}\right)$	
spot size	$w(z) = w_0 \sqrt{1 + \left(\frac{z}{z_0}\right)^2}$	
curvature of the phase front	$R(z) = z + \frac{z_0^2}{z}$	
Rayleigh length	$z_0 = \frac{\pi w_0^2}{\lambda}$	
waist size	$w_0$	

in the figure simple, we refer to just waist-size and waist position as the base of the modal expansion there].

The simulation in Figure 1 will go as follows. From the left, a field based on a base B1 goes into a substrate, and the field shape changes by the lensing effect of the substrate. A new base B2 is calculated on the right hand side of the substrate so that the incoming TEM<sub>00</sub> becomes a outgoing TEM<sub>00</sub> in the new base, or, the new base B2 is chosen so that the incoming field  $a_{00}U_{00}^{B1}$  becomes  $a_{00}U_{00}^{B2}$  after the lens. The field then interacts with the coating, or mirror, and some are reflected back to the left and some are transmitted into the cavity. The base of the reflected field is changed back to B1. The field in the cavity, going back and forth, is represented using base B2.

As is explained in this case, the simulation can start from the source with arbitrary base, then propagates down to the core optics. In reality, optics are arranged in between the laser and the core optics so that the mode matches at the core optics. What this means is that, in the example Figure 1 and the discussion above, the new base B2 is, ideally, the eigen state of the mode of the cavity defined by the two mirrors. To help this situation, the E2E package will provide a way to define the mode at the input which will match to the mode of the cavity when it goes into the core optics. The mode mismatches that occur due to small misalignments are, of course, what the E2E package simulates.

### 3.2.1. field is modified by mirror and lens and wedge

The base of Hermite\_Gaussian expansion can be represented by a complex number

$$q \equiv (z, -z_0)$$

This parameter is changed by mirror or lens in following ways:

### 3.2.1.1 A lens changes the base of Hermite-Gaussian expansion.

$$q_{out} = \frac{q_{in}}{1 - q_{in}/f}$$

where f is the focal length of lens.

The lens may also mix the components. E.g., thermal lensing effects.

Choice of the origin of z is relative to the waist position where guoy-phase (for all modes) equals to zero.

### 3.2.1.2 A mirror changes the mixture of components in the same expansion base.

- On reflection with normal incidence from a mirror,  $z \Rightarrow -z$  (by convention).
- On reflection with non-zero incidence angle from a mirror (different for bases in horizontal X and vertical Y direction, i.e., in the plane of incidence and perpendicular to plane of incidence respectively )

$$q_{outX} = \frac{q_{inX}}{1 - 2q_{inX}/(R \cos \theta)}$$

$$q_{outY} = \frac{q_{inY}}{1 - 2 \cos \theta q_{inY}/R}$$

### 3.2.2. Program to calculate the modal-base at the laser using the base defined by the pair of mirros in COC

In the following, we consider a simple case: a laser and a Fabry-Perot cavity. However, the same step-by-step method can be easily extended to more complicated set-up.

- Rayleigh range for the modal-base inside the cavity formed by two mirrors (mirror 1 is near to laser) :

$$Z_0 = \frac{\pi W_0^2}{\lambda} = \sqrt{\frac{L(R_1 - L)(R_2 - L)(R_1 + R_2 - L)}{(R_1 + R_2 - 2L)^2}}$$

Where R1 and R2 are absolute values of radii of curvature of two mirrors. Distances of the waist from mirror 1 and mirror 2 are respectively:

$$Z_1 = \frac{L(R_2 - L)}{R_1 + R_2 - 2L} \quad Z_2 = \frac{L(R_1 - L)}{R_1 + R_2 - 2L}$$

- At the input mirror 1 and inside the cavity, the radius of curvature of the beam wavwfront is,

of course,  $R_1$ . The half-width of the beam is:

$$W = W_0 \left[ 1 + \left( \frac{Z_1}{Z_0} \right)^2 \right]^{1/2}$$

- At the input mirror 1 and just outside the cavity, the radius of curvature of the beam (due to the lensing effect of mirror) is

$$R_{out} = \frac{R_1}{n}$$

where  $n$  is the refractive index of the mirror dielectric material (for fused silica,  $n=1.47$ ).

The change in the width size,  $W$ , after it passes through the mirror is assumed to be negligible.

- We are now ready to calculate modal-base for the laser from two known quantities: radius of curvature of beam wavefront,  $R_{out}$  and its width,  $W$  at the input mirror just outside the cavity. The waist-size for the new base and the distance of the (virtual) waist position from the input mirror are :

$$W_0(new) = \frac{WK}{\sqrt{1+K^2}} \quad Z = \frac{R_{out}}{1+K^2}$$

where

$$K = \frac{\lambda R_{out}}{\pi W^2}$$

### 3.3. Hermite-Gaussian modes

$H_m(x)$  is the Hermite polynomial of order  $m$ . The following relations are used repeatedly in the calculations which follow:

$$\int_{-\infty}^{\infty} U_m^\dagger(x, z) U_n(x, z) dx = \delta_{mn} \quad (0.1a)$$

$$2xH_m(x) = H_{m+1}(x) + 2mH_{m-1}(x) \quad (0.1b)$$

$$\frac{d}{dx}H_m(x) = 2mH_{m-1}(x) \quad (0.1c)$$

$$\int_{-\infty}^{\infty} U_m^\dagger(x, 0) \frac{H_i(\sqrt{2}x/w_0)}{H_k(\sqrt{2}x/w_0)} U_k(x, 0) dx = \sqrt{\frac{2^i i!}{2^k k!}} \delta_{mi} \quad (0.1d)$$

Eqn. (0.1a) is the orthonormality condition; eqns. (0.1b) and (0.1c) are recursion relations to be used to derive Hermite polynomials of any order, beginning with  $H_0(x) = 1$ .

In two dimensions the Hermite-Gaussian modes are given by

$$U_{mn} = U_m(x, z)U_n(y, z)e^{-ikz} \quad (0.2)$$

The explicit forma of a few low order Hermite polynomials are :

$$H_0(x) = 1; H_1(x) = 2x; H_2(x) = -2 + 4x^2; H_3(x) = -12x + 8x^3; \quad (0.3)$$

A few examples of the distribution of the Hermite Gaussians are shown below.

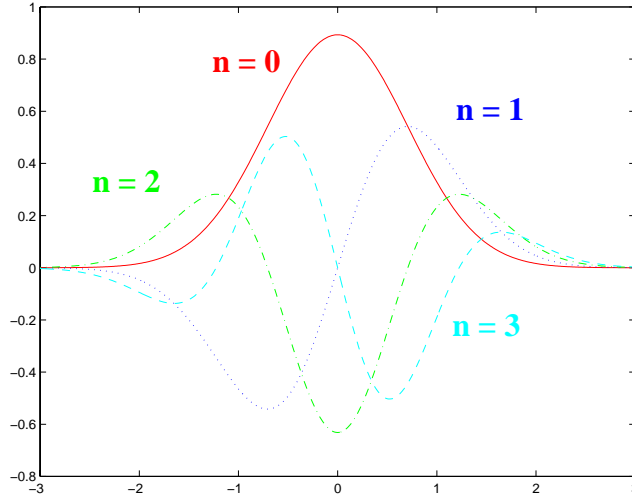


**Figure 2: HermiteGaussian**

The following formula is used in the modeling of the photo detector with simple shapes.

$$\int_0^{\infty} H_n(x)H_m(x) \exp(-x^2) dx$$

$$= \sum_{r=0}^{\lfloor \frac{n}{2} \rfloor} \sum_{s=0}^{\lfloor \frac{m}{2} \rfloor} (-1)^{r+s} \cdot \frac{n!m!2^{n+m-1}}{(2r)!!(2s)!!(n-2r)!(m-2s)!} \cdot \begin{cases} \left(\frac{n+m-1}{2} - r - s\right)! \cdot 2^{-r-s} & \text{for odd } n+m \\ \frac{(n+m-2r-2s-1)!!}{\sqrt{2}^{n+m}} \sqrt{\pi} & \text{for even } n+m \end{cases} \quad (0.4)$$

$$\text{Table 2: } HH[m, n] = \frac{1}{\sqrt{\pi}2^{m+n}m!n!} \int_0^{\infty} H_m(x)H_n(x)\exp(-x^2)$$

m \ n	0	1	2	3	4	5
0	$\frac{1}{2}$	$\frac{1}{\sqrt{2\pi}}$	0	$-\frac{1}{2\sqrt{3\pi}}$	0	$\frac{1}{4}\sqrt{\frac{3}{5\pi}}$
1	$\frac{1}{\sqrt{2\pi}}$	$\frac{1}{2}$	$\frac{1}{2\sqrt{\pi}}$	0	$-\frac{1}{4\sqrt{3\pi}}$	0
2	0	$\frac{1}{2\sqrt{\pi}}$	$\frac{1}{2}$	$\frac{1}{2}\sqrt{\frac{3}{2\pi}}$	0	$-\frac{1}{4}\sqrt{\frac{5}{6\pi}}$
3	$-\frac{1}{2\sqrt{3\pi}}$	0	$\frac{1}{2}\sqrt{\frac{3}{2\pi}}$	$\frac{1}{2}$	$\frac{3}{4\sqrt{2\pi}}$	0
4	0	$-\frac{1}{4\sqrt{3\pi}}$	0	$\frac{3}{4\sqrt{2\pi}}$	$\frac{1}{2}$	$\frac{3}{8}\sqrt{\frac{5}{2\pi}}$
5	$\frac{1}{4}\sqrt{\frac{3}{5\pi}}$	0	$-\frac{1}{4}\sqrt{\frac{5}{6\pi}}$	0	$\frac{3}{8}\sqrt{\frac{5}{2\pi}}$	$\frac{1}{2}$

$$\int_{-\infty}^{\infty} H_n(x)H_m(x)\exp(-x^2) = \begin{cases} \sqrt{\pi}2^n n! & \text{for } n=m \\ 0 & \text{for } n \neq m \end{cases} \quad (0.5)$$

## 3.4. Polarization

**3.4.0.1** At present the polarisation setting (p or s) in field is used just to determine the phase to be gained by a beam on reflection from the sides of a mirror. Capability of handling mixture of both polarization states has not yet been implemented.

**3.4.0.2** Mirrors have separate r and t for each polarization. Only one set of values (corresponding to only one polarisation) can be set for the current implementation.

**3.4.0.3** Our final implementation will take care of the above two restrictions (i) by doubling the number of field amplitudes carried by the “field” class (ii) by having two sets of reflectivity and

transmittivity values, each for one polarisation.

## 4 VINET'S ALGEBRA FOR MISALIGNMENT CALCULATION

In this chapter we present the modal model approach to the study of misalignment in LIGO interferometer (represented by the subclasses of “complex\_matrix” class in e2e) and a fast algorithm (represented by “align\_smart” class in e2e). This fast algorithm is based on “A\_266 algebra” developed by Cavalier, Hello and Vinet for VIRGO. In e2e, however, we extend the same algebra to third order (thus, A\_3-10-10) to make our calculation more accurate by including 10 basic TEM modes. In general, an expansion upto n-th order corresponds to the inclusion of  $(n+1)(n+2)/2$  number of modes. The in-built characteristics of “align-smart” class allow us to easily extend our scope of computation to any higher order, provided the misalignment parameters remain within the limit where modal model remains to be a valid description (e.g. in case of the rotation of mirrors, pitch or yaw value should remain small as compared to the divergence of beam which is about 10 microrad for LIGO). We will see that the inclusion of modes only upto second or third order is sufficient to serve most of our purpose in initial LIGO interferometers.

If the series expansion is limited to third order in parameters p and q, the rotation matrix is a square matrix of dimension 10. The zeroth order terms form a unit matrix as in Fig.1. This basically means that, in absence of any rotation of mirror, all the 10 modes considered get either reflected or transmitted without suffering any relative change with respect to each other (there's of course a uniform attenuation by reflection or transmission factor).

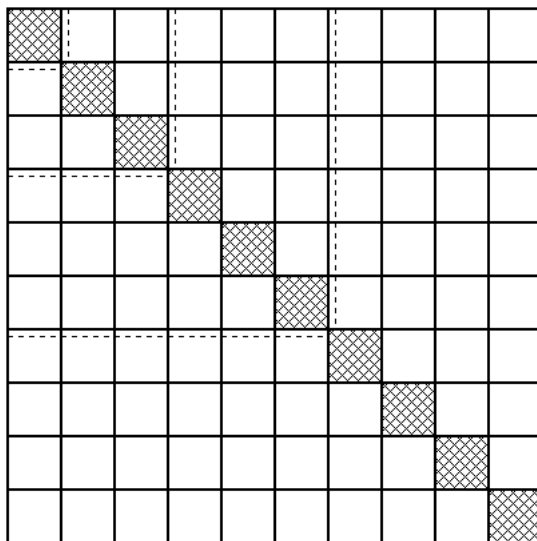


**Figure 3:** The Mosaic for zeroth order terms in a A3-10-10 matrix

For an expansion upto third order in parameters p and q, there are 18 non-zero first order terms forming a mosaic as in Fig.2. The terms are:

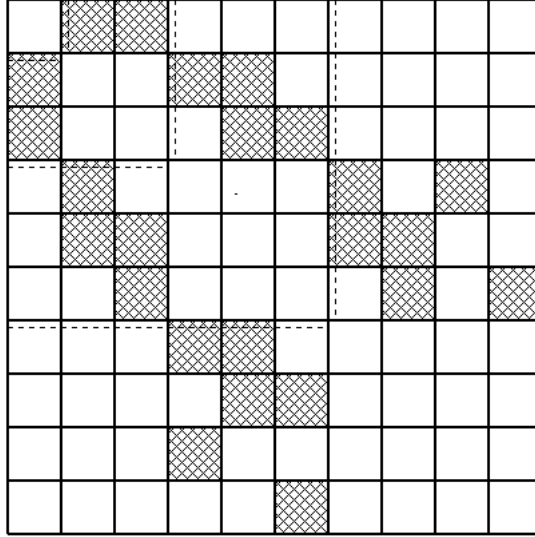


**Figure 4:** The Mosaic for first order terms in a A3-10-10 matrix

$$R_{01} = R_{10} = R_{24} = R_{42} = R_{57} = R_{75} = i \frac{p}{\sqrt{2}}$$

$$R_{02} = R_{20} = R_{14} = R_{41} = R_{36} = R_{63} = i \frac{q}{\sqrt{2}}$$

$$R_{13} = R_{31} = R_{46} = R_{64} = ip$$

$$R_{25} = R_{52} = R_{47} = R_{74} = iq$$

$$R_{38} = R_{83} = ip\sqrt{1.5}$$

$$R_{59} = R_{95} = iq\sqrt{1.5}$$

The number of non-zero second order terms (if we consider expansion only upto third order in parameters p and q) is 40. Fig.3 presents the mosaic formed by these and the actual terms are presented below:

$$R_{00} = -0.25(p^2 + q^2) \quad R_{11} = -0.25(3p^2 + q^2)$$

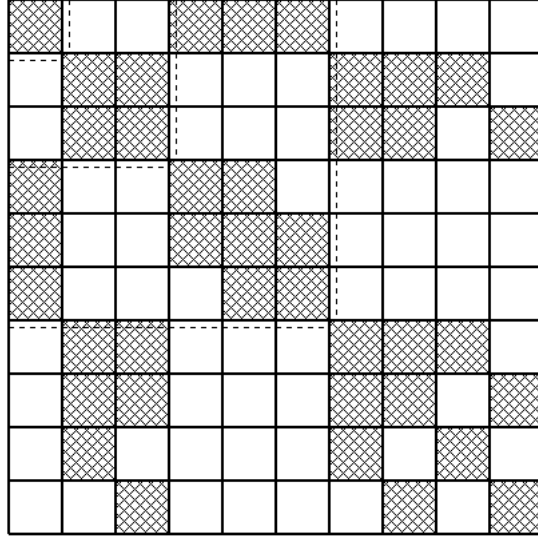


**Figure 5:** The Mosaic for second order terms in a A3-10-10 matrix

$$R_{22} = -0.25(p^2 + 3q^2) \quad R_{33} = -0.25(5p^2 + q^2)$$

$$R_{44} = -0.75(p^2 + q^2) \quad R_{55} = -0.25(p^2 + 5q^2)$$

$$R_{66} = -0.25(5p^2 + 3q^2) \quad R_{77} = -0.25(3p^2 + 5q^2)$$

$$R_{88} = -0.25(7p^2 + q^2) \quad R_{99} = -0.25(p^2 + 7q^2)$$

$$R_{03} = R_{30} = R_{26} = R_{62} = -\frac{p^2}{2\sqrt{2}} \quad R_{18} = R_{81} = -\frac{\sqrt{6}}{4}p^2$$

$$R_{05} = R_{50} = R_{17} = R_{71} = -\frac{q^2}{2\sqrt{2}} \quad R_{29} = R_{92} = -\frac{\sqrt{6}}{4}q^2$$

$$R_{67} = R_{76} = -pq \quad R_{04} = R_{40} = R_{12} = R_{21} = -\frac{pq}{2}$$

$$R_{68} = R_{86} = R_{79} = R_{97} = -\frac{\sqrt{3}}{2}pq$$

$$R_{16} = R_{61} = R_{27} = R_{72} = R_{34} = R_{43} = R_{45} = R_{54} = -\frac{pq}{\sqrt{2}}$$

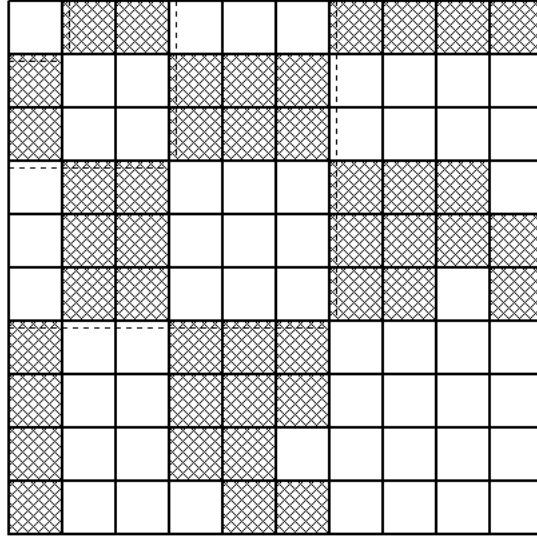


**Figure 6:** The Mosaic for third order terms in a A3-10-10 matrix

There are 44 third order terms, if we limit our expansion only upto third order in parameters p and q. These form a mosaic as in Fig.4. The terms are:

$$R_{08} = R_{80} = -\frac{i}{4}p^3 \quad R_{09} = R_{90} = -\frac{i}{4}q^3$$

$$R_{06} = R_{60} = R_{23} = R_{32} = -\frac{i}{4}p^2q$$

$$R_{07} = R_{70} = R_{15} = R_{51} = -\frac{i}{4}pq^2$$

$$R_{37} = R_{73} = -\frac{i}{2\sqrt{2}}pq^2 \quad R_{56} = R_{65} = -\frac{i}{2\sqrt{2}}p^2q$$

LIGO-DRAFT

$$R_{48} = R_{84} = -i\frac{\sqrt{3}}{4}p^2q \quad R_{49} = R_{94} = -i\frac{\sqrt{3}}{4}pq^2$$

$$R_{01} = R_{10} = -\frac{i}{4\sqrt{2}}(p^3 + pq^2) \quad R_{02} = R_{20} = -\frac{i}{4\sqrt{2}}(q^3 + p^2q)$$

$$R_{13} = R_{31} = -\frac{i}{4}(2p^3 + pq^2) \quad R_{25} = R_{52} = -\frac{i}{4}(2q^3 + p^2q)$$

$$R_{46} = R_{64} = -\frac{i}{4}(2p^3 + 3pq^2) \quad R_{47} = R_{74} = -\frac{i}{4}(2q^3 + 3p^2q)$$

$$R_{38} = R_{83} = -i\frac{3}{4\sqrt{6}}(3p^3 + pq^2) \quad R_{59} = R_{95} = -i\frac{3}{4\sqrt{6}}(3q^3 + p^2q)$$

$$R_{24} = R_{42} = -\frac{i}{4\sqrt{2}}(p^3 + 3pq^2) \quad R_{14} = R_{41} = -\frac{i}{4\sqrt{2}}(q^3 + 3p^2q)$$

$$R_{57} = R_{75} = -\frac{i}{4\sqrt{2}}(p^3 + 5pq^2) \quad R_{36} = R_{63} = -\frac{i}{4\sqrt{2}}(q^3 + 5p^2q)$$

These mosaics form a complete algebraic set among themselves.

## 5 DETECTOR, DEMODULATION AND SHOTNOISE

### 5.1. Detector matrix

Using the expression defined in Section 8.2.2., the power observed by a detector located at a given  $z$  position is given by the following expression. In this calculation,  $\exp(-ir^2(k_0+k_i)/R)$  is approximated by  $\exp(-ir^2k_0/R)$ , because the correction is of the order of  $\lambda_{CR}/\lambda_{SB} \sim 10^{-7}$ .  $D(x,y)$  is a pupil-weighting function, and  $\Omega$  is the area of the photodetector. As can be seen from Eq.(5), a detector can be characterized by a detector matrix  $D_{mn,m'n'}$ .

$$\begin{aligned}
P &= \int_{\Omega} dx dy |E(x, y, z, t)|^2 \cdot D(x, y) \\
&= \sum_{m, n, m', n'} E^{mn}(z, t) \cdot E^{m'n'}(z, t)^{\dagger} \cdot D_{mn, m'n'}
\end{aligned} \tag{5}$$

$$E^{mn}(z, t) = \sum_i \exp(i\Omega_i t) \cdot \tilde{E}_i^{mn}(t) \tag{6}$$

$$\begin{aligned}
D_{mn, m'n'} &= \int_{\Omega} dx dy U_{mn}(x, y, z) \cdot U_{m'n'}(x, y, z) \cdot D(x, y) \\
&= d_{mn} d_{m'n'} \cdot \int_{\Omega} dx dy e^{-(\hat{x}^2 + \hat{y}^2)} H_m(\hat{x}) H_{m'}(\hat{x}) H_n(\hat{y}) H_{n'}(\hat{y}) D(\hat{x}, \hat{y})
\end{aligned} \tag{7}$$

$$= \frac{1}{2} d_{mn} d_{m'n'} \cdot \int_{\rho_{min}}^{\rho_{max}} d\rho \int_{\Phi_{min}}^{\Phi_{max}} d\phi H_m(\hat{x}) H_{m'}(\hat{x}) H_n(\hat{y}) H_{n'}(\hat{y}) D(\hat{x}, \hat{y})$$

$$d_{mn} = \frac{1}{\sqrt{\pi 2^{m+n} m! n!}}$$

$$\hat{r} = \frac{r}{w(z)} \quad \hat{x} = \frac{\sqrt{2}}{w(z)} x = \hat{r} \cos(\phi) \quad \hat{y} = \frac{\sqrt{2}}{w(z)} y = \hat{r} \sin(\phi) \tag{8}$$

$$\rho_{min} = \exp(-\hat{r}_{max}^2) \quad \rho_{max} = \exp(-\hat{r}_{min}^2)$$

In the simulation package, if the detector matrix cannot be calculated analytically using formulas in the Appendix, the matrix is calculated numerically.

## 5.2. Demodulation

By substituting the explicit frequency dependence eq.(6) to eq.(5), the expression of the power in a detector can be rewritten in the following way.

LIGO-DRAFT

$$\begin{aligned}
P &= \sum_{i,j} P_{ij} \cdot \exp(i(\Omega_i - \Omega_j)t) \\
&= \sum_i P_{ii} + \sum_{i < j} (P_{ij} \exp(i\Delta_{ij}t) + \text{c.c.}) \\
&= \sum_i P_{ii} + 2 \sum_{i < j} ((-P_{ij}^{Im}) \sin(\Delta_{ij}t) + P_{ij}^{Re} \cos(\Delta_{ij}t))
\end{aligned} \tag{9}$$

$$P_{ij} = \sum_{m,n,m',n'} \tilde{E}_i^{mn}(t) \cdot \tilde{E}_j^{m'n'}(t)^\dagger \cdot D_{mn,m'n'} = P_{ij}^{Re} + iP_{ij}^{Im} \tag{10}$$

$$\Delta_{ij} = \Omega_i - \Omega_j \tag{11}$$

The CD part of the power is given by the first term in eq.(9),

$$P_{DC} = \sum_i P_{ii} \tag{12}$$

The conversion of the phase modulation adopted in this simulation is

$$E_{modulated} = E_{in} \exp(i\Gamma \sin(\Omega \cdot t)) \tag{13}$$

When the photo diode current is demodulated using a sinusoidal wave with the demodulation frequency of  $\Delta\Omega$ , the inphase and quad phase demodulated amplitudes are given as follows:

$$P_{In} = \frac{1}{T} \int_0^T P(t) \sin(\Delta\Omega \cdot t) = \sum_{\Omega_i - \Omega_j = \Delta\Omega} (-P_{ij}^{Im}) \tag{14}$$

$$P_{Qu} = \frac{1}{T} \int_0^T P(t) \cos(\Delta\Omega \cdot t) = \sum_{\Omega_i - \Omega_j = \Delta\Omega} (P_{ij}^{Re}) \tag{15}$$

### 5.3. shot noise

Because of the quantum nature of the electric field, the measured current of the photo diode fluctuates around the expected value. For a given input field power  $P(t)$ , the average number of photons for a measured time interval  $\Delta t$  is given by the following formula

$$n_0(t) = \frac{e_0(t)}{h \cdot \nu} = \frac{\eta \cdot P(t) \cdot \Delta t}{h \cdot \nu} \tag{16}$$

where  $h\nu$  is the energy of a photon and  $\eta$  is the quantum efficiency of the detector. The measured number of photons fluctuates randomly following the poisson distribution with the given average value.  $\aleph(n)$  is used to denote a number observed with the average value of  $n$ .

When a measurement is done for a time interval of  $\tau$  using a modulation frequency  $\Omega=2\pi/T$ , the power, inphase and quad phase demodulated signals are given by the following expressions, where the integration over time is replaced by a summation with a time step of  $\Delta t$ .

$$\bar{P}_x^{obs} = \frac{1}{\tau} \int_0^{\tau} w_x(t) P^{obs}(t) dt = \frac{1}{n_b n_c \Delta t} \sum_{i=1}^{n_b} \sum_{j=1}^{n_c} w_x(t_i^j) h\nu \aleph(n_0(t_i^j))$$

$$w_{DC}(t) = 1 \quad w_{In}(t) = \sin(\Omega \cdot t) \quad w_{Qu}(t) = \cos(\Omega \cdot t) \quad (17)$$

$$n_b = \frac{T}{\Delta t} \quad n_c = \frac{\tau}{T} \quad t_i^j = (i + n_b \cdot j) \Delta t$$

$n_c$  is the total number of oscillations in the observation period, and  $n_b$  is the number of binning

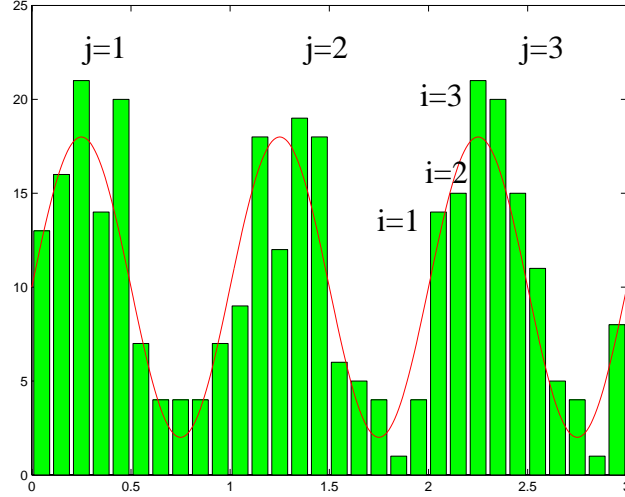


**Figure 7: Quantized power ( $n_b=10, n_c=3$ )**

per oscillation. If the time dependence of the field, or  $P_{ij}$  in eq.(10), is neglected during the measurement period  $\tau$ ,  $\aleph(n)$  and  $w_x(t_i^j)$  are independent of the cycle, or  $j$ , and eq.(17) can be rewritten in the following way.

$$\bar{P}_x^{obs} = \frac{1}{n_b \cdot \Delta t} \sum_{i=1}^{n_b} w_x(t_i) \frac{h\nu \aleph(n_c \cdot n_0(t_i))}{n_c}$$

$$t_i = i\Delta t \quad (18)$$

## **6 SECTION 1SUMMATION CAVITIES (FAST ALGORITHM)**

### **6.1. Fabry-Perot Cavity**

### **6.2. Recycled Michelson Cavity**

### **6.3. Triangular Cavity**

## **APPENDIX 1 REFERENCES**

[1]

[2]

**LIGO-DRAFT**